Highly stretchable, elastic, and ionic conductive hydrogel for artificial soft electronics

Zhou, Yang; Wan, Changjin; Yang, Yongsheng; Yang, Hui; Wang, Shancheng; Dai, Zhendong; Ji, Keju; Jiang, Hui; Chen, Xiaodong; Long, Yi

2019

Zhou, Y., Wan, C., Yang, Y., Yang, H., Wang, S., Dai, Z., . . ., Long, Y. (2018). Highly stretchable, elastic, and ionic conductive hydrogel for artificial soft electronics. Advanced Functional Materials, 29(1), 1806220-. doi:10.1002/adfm.201806220

https://hdl.handle.net/10356/137817

https://doi.org/10.1002/adfm.201806220

WILEY-VCH

DOI: 10.1002/ ((please add manuscript number))
Article type: Full Paper

Highly Stretchable, Elastic, and Ionic Conductive Hydrogel for Artificial Soft Electronics

Yang Zhou, Changjin Wan, Yongsheng Yang, Hui Yang, Shancheng Wang, Zhendong Dai, Keju Ji, Hui Jiang, Xiaodong Chen, and Yi Long**

Dr. Y. Long School of Materials Science and Engineering, Nanyang Technological University, 50 Nanyang Avenue, 639798, Singapore
Singapore-HUJ Alliance for Research and Enterprise (SHARE), Nanomaterials for Energy and Energy-Water Nexus (NEW), Campus for Research Excellence and Technological Enterprise (CREATE), 138602, Singapore
E-mail: longyi@ntu.edu.sg

Prof. X. Chen School of Materials Science and Engineering, Nanyang Technological University, 50 Nanyang Avenue, 639798, Singapore
Singapore-HUJ Alliance for Research and Enterprise (SHARE), Nanomaterials for Energy and Energy-Water Nexus (NEW), Campus for Research Excellence and Technological Enterprise (CREATE), 138602, Singapore
Innovative Center for Flexible Devices (iFLEX), School of Materials Science and Engineering Nanyang Technological University, 50 Nanyang Avenue 639798, Singapore
E-mail: chenxd@ntu.edu.sg

Y. Zhou, Dr. C. Wan, Dr. H. Yang, S. Wang, Dr. H. Jiang School of Materials Science and Engineering, Nanyang Technological University, 50 Nanyang Avenue, 639798, Singapore

Dr. Y. S. Yang School of Chemistry and Engineering, Wuhan Textile University, 1 Textile Road, 430073, Wuhan, China

Prof. Z. Dai, Prof. K. Ji Institute of Bio-Inspired Structure and Surface Engineering, Nanjing University of Aeronautics and Astronautics, 29 Yudao Street, 210016, Nanjing, China

Dr. C. Wan Innovative Center for Flexible Devices (iFLEX), School of Materials Science and Engineering Nanyang Technological University, 50 Nanyang Avenue 639798, Singapore

Keywords: Tough hydrogel, ionic conductive hydrogel, soft electronics, bioelectronics, tissue engineering

Abstract

High conductivity, large mechanical strength and elongation are important parameters for soft electronic applications. However, it is difficult to find a material with balanced electronic and mechanical performance. Here, a simple method was developed to introduce ions rich pores into strong hydrogel matrix and fabricate a novel ionic conductive hydrogel with a high level of electronic and mechanical properties. Our proposed ionic conductive hydrogel was achieved by physically cross-linking the tough biocompatible polyvinyl alcohol (PVA) gel as the matrix and embedding hydroxypropyl cellulose (HPC) bio-polymer fiber inside matrix followed by salt solution soaking. The wrinkle and dense structure induced by salting in PVA matrix provides large stress (1.3 MPa) and strain (975%). The well-distributed porous structure as well as ionic migration facilitated ion-rich environment generated by embedded HPC fibers dramatically enhance ionic conductivity (up to 3.4 S m^{-1}, at f = 1 MHz). The conductive hybrid hydrogel can work as an artificial nerve in three-dimensional (3D) printed robotic hand, allowing passing stable and tunable electrical signals and full recovery under robotic hand finger movements. This natural rubber like ionic conductive hydrogel has a promising application in artificial flexible electronics.

1. Introduction

Stretchable and flexible electronics have been received increasing attention due to their unique advantages and wide applications in the fields of biomedicine, soft robotics, energy harvesting, etc.[1] For the biological applications, the stretchable materials need to integrate superior performance of both high conductivity and good mechanical properties so that they can be suitable for the long-time biocompatible use with human bodies such as skin, muscle, heart, or brain.[2] In addition to the demands of high conductivity and good stretchability, some important parameters should also be carefully considered for a specific application, for example, the conductors may need to operate at high frequencies, be biocompatible and remain conductive while undergoing high expansions,[3] whereas the existing electronic conductors struggle to

meet these demands. It is still a challenge to fabricate such systems with desirable multiple functions.

Hydrogel is a kind of 3D polymeric network which could swell in water.[4] The polymer networks of the hydrogel make it solid-like while the aqueous phase of the hydrogel enables fast diffusion of the carriers, which indicates the hydrogels have liquid-like transport properties. Due to these good attributes, many hydrogels are biocompatible and soft, making them perfect candidates for applications of biocompatible materials,[5] drug delivery,[6] energy saving,[7] medical dressings,[8] tissue engineering,[9] etc. However, the poor mechanical strength and strain of hydrogel seriously limit its potential applications.[10] Recently, toughening hydrogels were fabricated to increase the stretchability and toughness by adding nanoparticles[11] and double networking.[12] The mechanical properties of toughening hydrogels were improved. However, the improvements are too low to reach the level of natural rubbers.[13] It is necessary to increase the mechanical properties further as well as keep high conductivity so that we can make the hydrogels work with soft human tissues, such as muscle and skin.[14]

With increasing of the crosslink density, the mechanical strength and the elasticity of the hydrogels will increase[15] while the resistance of the ion migration will also increase,[16] so it is hard to keep both high mechanical strength and high ionic conductivity at the same time. The ionic conductive gel is a possible solution since it can keep high conductivity via ion transport while the high toughness can be provided by the large strain, but the mechanical strength and elasticity were relatively low.[17] For example, Odent *et al.* fabricated an ionic conductive gel with high conductivity of 2.9 S m^{-1} and a large strain of 425% demonstrated, but the tensile strength and elasticity were relatively low as 0.007 MPa and 5 kPa, respectively.[18] However, for real commercial applications, high mechanical strength is required for conductive hydrogels in stretchable sensor and artificial tissue applications to bear enormous mechanical loads and avoid unexpected fractures.[19] At the same time, the mechanical properties of designed materials should mimic tissue without compromising its high conductivity because the

mismatch between artificial materials and tissues may cause further scarring by immunological responses.[20] Thus, the balanced mechanical strength, elongation, and elasticity to human tissue with high conductivity are important for stretchable soft artificial materials, but hard to be achieved at the same time.

In this manuscript, we demonstrated a novel method to fabricate a natural rubber-like ionic conductive hydrogel. Biocompatible Hydroxypropyl cellulose (HPC)[21] embedded physical-crosslinked polyvinyl alcohol (PVA) hydrogel[22] were infiltrated into the sodium chloride (NaCl) solution and formed an HPC/PVA ionic conductive hydrogel. This natural rubber-like HPC/PVA ionic conductive hydrogel was easily turned its mechanical properties and ionic conductivities to match different soft tissues requirements by turning HPC fibers' concentration (from 0 to 3.75 wt%) and NaCl solution soaking level (from 1 to 5M solution). This natural rubber-like HPC/PVA hydrogel is biocompatible, stretchable (fully recover under 100% strain), and combines tunable mechanical strength (from 0.6 to 4 MPa tensile strength) and elasticity (from 15 to 900 kPa), large strain (up to 975%), and high ionically conductivity (up to 3.4 S m^{-1} at f = 1 MHz). In this hydrogel, the stiff and dense PVA hydrogel was selected to provide large mechanical strength after soaking in a salt solution. The embedded HPC fibers enhanced ionic conductivity, while turning the mechanical properties at the same time. We demonstrated the natural rubber like HPC/PVA ionic conductive hydrogel as artificial ligament and nerve in a 3D printed robotic hand. With strain increased from 0 to 100%, the alternative current signal changes were negligible at high frequency, which means it can transfer steady AC signal under expansion and could act as a monitor with muscle movement. This ionic conductive hydrogel can also work together with a pressure sensor as artificial nerve to transfer touch signal (DC signal) with different finger positions (different strains), which will generate different touch signals.

2. Results and Discussion

2.1. Synthetic strategy and mechanism investigation

Considering the good mechanical strength and high water retaining ability as well as the good biocompatibility and flexibility in artificial soft tissue applications,[23] PVA hydrogel is carefully selected to fabricate the new ionic conductive hydrogel. HPC fiber is selected to be embedded into PVA hydrogel to enhance the ions concentration after soaking in NaCl solution since it can attract both Na^+ and Cl^- ions in solution. In order to synthesize rubber-like ionic conductive HPC/PVA hydrogel, physically crosslinked PVA hydrogels with embedded HPC fibers are firstly fabricated. The embedded HPC fibers inside PVA hydrogels matrix will decrease the crosslinking density of PVA hydrogel matrix and generate water rich porous area. After soaking HPC/PVA hybrid hydrogels in NaCl solution, Na^+ and Cl^- ions will diffuse into HPC/PVA hybrid hydrogels and water molecules will diffuse out from HPC/PVA hydrogels to reach balanced ionic concentration. At the same time, HPC fibers will attract more ions[24] to water rich porous area. The HPC/PVA hybrid hydrogels will become conductive due to the absorption of Na^+ and Cl^- ions. The mechanical properties of HPC/PVA ionic conductive hydrogel is supposed to be enhanced because of the salting out effect of Na^+ and Cl^- ions. Both mechanical properties and ionic conductivity are expected to be tuned by changing the soaking level from 1 to 5M.

Figure 1 shows the schematic illustration, microstructure structure and microscope photos of pure PVA hydrogel, HPC/PVA hybrid hydrogel and HPC/PVA ionic conductive hydrogel after soaking in NaCl solution. Pure PVA hydrogel exhibits the uniform structure (Figure 1a), and no porous structure or defects can be observed as seen in Figure 1a (iii). Once HPC short-chain fibers were introduced into PVA hydrogel system, the fibers in HPC/PVA hydrogel were well distributed and generated water-rich pores (Figure 1b (i)), which is due to HPC short chains dispersed in between PVA polymer chains (Figure 1b (ii)) without interaction (**Figure S1** shows

FTIR spectrum of commercial PVA powders, HPC fibers and dried HPC/PVA hydrogel, no new significant peaks generated after HPC/PVA hydrogel obtained). The pores were suggested to be filled with HPC solution, as HPC solution was kept liquid state during HPC/PVA gelation process (**Figure S2**).As shown in Figure 1b (iii), the water-rich porous area can be observed inside the uniform PVA hydrogel matrix. With HPC content increasing, number of pores was also increasing (**Figure S3**). After soaking HPC/PVA hydrogel in NaCl solution, the pores in HPC/PVA ionic conductive hydrogel became Na^+ and Cl^- ions rich area, due to ions diffusion and the attraction of HPC chains to salt ions[62] (Figure 1c (i), (ii)). The porous structure can be straightly observed through microscope (Figure 1c (iii)). The whole hydrogel shrunk (**Figure S4**) due to the salting out effect, meanwhile, PVA polymer chains became densely packed with wrinkle structure generated (**Figure S5**). Figure S3a, b show the height distribution detected by optical surface profiler of HPC/PVA hydrogel before and after soaking in NaCl solution (5M), respectively. Wrinkles structure looks like "mountain ridge" that can be observed in Figure S4b.

2.2. Mechanical properties of HPC/PVA ionic conductive hydrogel

The HPC/PVA_x composite hydrogels were obtained with different PVA amount (x refers to the weight percentage of PVA compared with a solution, i. e. 8, 16 and 24%) and a fixed HPC weight percentage at 2.5 wt%. Soaked in sodium chloride (NaCl) solution (3M, 24 hours), the mechanical strength of composite hydrogels increases with x increasing, while HPC/$PVA_{16\%}$ ionic conductive hydrogel provides the highest strain and toughness (**Figure 3**a) as HPC amount is fixed at 2.5 wt% (weight percentage of HPC compared with solution). Compared with pure $PVA_{16\%}$ ionic conductive hydrogel of same PVA/H_2O ratio and soaking level, HPC/$PVA_{16\%}$ ionic conductive hydrogel exhibits more suitable tensile strength, elasticity and toughness (Figure 2a). The extremely large Young's modulus (900 kPa) of pure $PVA_{16\%}$ ionic conductive hydrogel limited its usage in artificial tissue application, due to the elasticity mismatch with human tissue (around 5 to 1000 kPa).[14] According to Figure 2a, HPC plays a

vital role in this ionic conductive hydrogel, which successfully increases the strain and decreases Young's modulus in comparison to pure PVA hydrogel.

$HPC/PVA_{16\%}$ hydrogel was selected to fabricate ionic conductive hydrogel (HPC/PVA hydrogel represents $HPC/PVA_{16\%}$ hydrogel in the following article). By adjusting the concentration of NaCl solution, mechanical properties of the ionic conductive hydrogels was facilely tuned (**Figure S6**). Figure 2b and c show that after the ionic conductive hydrogel soaked in different concentration of NaCl solution from 1M to 5M, the largest tensile strength reaches 1.3±0.2 MPa after soaking in 5M solution, which was 13 times higher than that of the original hydrogel without soaking (0.1 MPa). At the same time, the largest strain reaches 8.6±1.2 after 2M NaCl solution soaking, which is 3 times higher than that of the original strain. HPC/PVA ionic conductive hydrogel exhibited a suitable elastic modulus from 95.8±12.1 kPa to 586.7±14.9 kPa (Figure 2d). The toughness dramatically increased 42 times from 0.139±0.1 MJ m^{-3} for $HPC/PVA_{16\%}$ original hydrogel to 5.85±0.8 MJ m^{-3} after soaking in 3M solution (Figure 2e) and this particular ionic conductive hydrogel was further demonstrated to stand various deformations such as, elongation, knotting and compression, which exhibits both superior stiffness as well high toughness (Figure 2f, g, h). Notably, the ionic conductive hydrogels could recover to their original shape after removing pressure, indicating its outstanding shape-recovery performance (Figure 2h). Due to the high mechanical strength, this 2×5 mm ionic conductive hydrogel could bear 2.5 kg weight as shown in **Figure S7** without perceptible crack or fracture.

The remarkable improvement of mechanical properties of HPC/PVA ionic conductive hydrogel before and after soaking was mainly provided by PVA matrix, which could be ascribed to three possible reasons. Firstly, as depicted in Figure 1, the salting-out effect decreases the volume of HPC/PVA hydrogel (Figure S4), which directly increased the density of the PVA matrix. Secondly, the wrinkle morphology (Figure S5b) due to the shrinkage enables the ionic conductive hydrogels to perform larger strain than the original HPC/PVA hydrogel under

tensile stress to toughen the ionic conductive hydrogels. **Figure S8** showed the SEM image of freeze-dried HPC/PVA hydrogel after soaking in NaCl solution, a large area of wrinkle structure can be observed (NaCl crystals observable on the cutting surface after freeze drying). The increasing of microcrystallites in HPC/PVA hydrogel after soaking was the third potential reason of toughness enhancement. **Figure S9** shows the XRD spectra of HPC/PVA, and HPC/PVA ionic conductive hydrogels with different concentration NaCl solution soaking and the peaks at 19° represents the microcrystallites of PVA hydrogel.[25] As the NaCl concentration increases, the intensity of microcrystallite peaks increases, which may enhance the toughness of HPC/PVA ionic conductive hydrogel.

2.3. Electrical properties of HPC/PVA ionic conductive hydrogel

The conductivity of HPC/PVA ionic conductive hydrogel was enhanced by introducing a porous structure through embedding HPC second network compared with pure PVA ionic conductive hydrogel. As HPC ratio increasing from 0 to 3.75 wt%, ionic conductivity increased from 1.7 to 3.4 S m^{-1} (f = 1 MHz, NaCl solution soaking level is 5M) (**Figure 3**a). The morphology of the HPC/PVA ionic conductive is finely tuned by using different concentrations of HPC. Higher HPC concentration implies more porous in the PVA network, which can be confirmed from the optical microscope (Figure S2 shows the porous distribution in HPC/PVA hydrogel increasing as HPC ratio increasing from 0 to 3.75 wt%). Therefore, HPC/PVA ionic conductive hydrogel with a higher concentration of HPC that possesses more pores, which would absorb more ions and provide more space to facilitate ionic migration.[26] These porous endow the hydrogel with high ionic conductivity while weakening the mechanical properties (**Figure S10**) due to the introduction of pores (defects). As a compromised result, HPC/PVA ionic conductive hydrogel with 2.5 wt% HPC ratio is selected in this work to analyze soaking level effect, considering the relatively high ionic conductivity up to 2.6 S m^{-1}, as well as the suitable mechanical properties (1.3 MPa tensile, 520% strain and 590 kPa Young's modulus).

As shown in Figure 3b, HPC/PVA ionic conductive hydrogels (2.5 wt% HPC ratio) are sensitive to strain with direct current (DC) applied and the gauge factor increases as strain increases from 0 to 400%. At the same time, with increasing soaking level, the gauge factor of hydrogels decreases.

Next, the conductive properties of the ionic conductive hydrogel under AC signal were investigated (Figure 3c). The conductivity increases with increased frequency at the same soaking level. At the same time, the conductivity also increases with the increased soaking level at the fixed frequency, due to the higher ionic concentration. Compared with pure PVA hydrogel, the electronic conductivity HPC/PVA ionic hydrogel at same soaking level is nearly doubled (2.6 vs. 1.3 S m^{-1} at f = 1 MHz). As shown in the EDX results of Na^+ and Cl^- elements in both HPC/PVA (**Figure S11a, b**) and pure PVA (Figure S11c, d) ionic conductive hydrogel after freeze-drying, ions was uniformly distributed in both hydrogel, and the content of both Na^+ and Cl^- ions in HPC/PVA hydrogel are higher than that of pure PVA hydrogel. Such high conductivity of the hydrogel under the alternating electric field could enable the high efficiency of electric signal transmission in soft electronic devices in artificial tissue.

To study the AC resistance characteristics under strain, a simple test circuit was used as shown in **Figure S12**. One ionic conductive hydrogel film (5.5 cm ×1.2 cm × 0.2 cm) was connected with a resistor (R1=4.67 kΩ) in series. 1.0 V sigmoidal signals (VI) were applied on the hydrogel wire and the resistor, then the voltage response on the hydrogel (VO) was measured as an output. By varying the strain applied on hydrogel from 0 to 100%, slight changes in voltage output could be observed with AC signal of both 1 kHz (human muscle electronic signal frequency is from 10^{-1} to 10^3 Hz)[27] and 1 MHz, as shown in **Figure S13a** and b, respectively. The voltage changes could be considered as the changes in resistance when loading a strain on the hydrogel and the resistance of the hydrogel could be estimated by the equation: $R_{gel}=R_1*U_O/(U_I-U_O)$. The relative change in resistance was plotted as a function of strain as shown in Figure 3d. A similar trend could be found with the two frequencies, in which low

resistance change could be observed by increasing the strains. Low gauge factor of 0.947 and 0.984 were achieved for 1 MHz and 1 kHz signals respectively (**Figure S14**). The mechanical properties make the HPC/PVA ionic conductive hydrogels promising for artificial tissue applications.

According to the test results of mechanical and electrical properties, both HPC concentration and NaCl soaking level will affect the mechanical and electrical properties of HPC/PVA ionic conductive hydrogels. As HPC concentration increased, both tensile strength and Young's modulus of HPC/PVA ionic conductive hydrogels were reduced, while ionic conductivity was increased at a fixed soaking level. Once the NaCl solution soaking level increased, all of the mechanical strength, elasticity and conductivity were increased. At the same time, water content reduced with soaking level increasing (**Figure S15a**), which result in the reduction of conductivity increasing rate (Figure S15b).

2.4. Demonstration of HPC/PVA ionic conductive hydrogel as artificial tissue

Compared with recently generated ionic conductive gels,[18, 28] this new HPC/PVA ionic conductive hydrogel combined high ionic conductivity, balanced tensile strength and strain, as shown in **Figure 4**. HPC/PVA ionic conductive hydrogel with 5M NaCl soaking level gives the best electronic conductivity, and HPC/PVA ionic conductive hydrogel with 3M NaCl soaking level showed the best mechanical property. Such results indicate our ionic conductive hydrogel possess the high potential for the tissue monitor and replacement. Furthermore, to well match other soft functional components, Young's modulus and toughness are other important parameters. Normally Young's modulus and toughness of hydrogel-based artificial tissue range from 10 to 1750 kPa and 0.1 to 12 MJ m^{-3},[29] respectively. According to **Figure S16**, both HPC/PVA ionic conductive hydrogel with 3M and 5M soaking level have suitable Young's modulus (250 and 650 kPa) and large toughness (6.7 and 5.8 MJ m^{-3}) compared with other reported artificial tissue hydrogels. HPC/PVA ionic conductive hydrogel with 5M NaCl

soaking level was selected to fabricate artificial tissues for the following demonstration due to its higher conductivity (Figure 4).

The HPC/PVA ionic conductive 5M hydrogel shows good self-recovery at 100% strain (**Figure 5**a and **Video 1**). As discussed above, the conductivity of this hydrogel is steady under strain from 0 to 100%. We further demonstrated this hydrogel as artificial ligament on a 3D printed robotic hand with steady 1 kHz AC at 10 V with the circuitry (**Figure S17**). This ionic conductive hydrogel with a length of 15 cm was connected to the cathode of a LED, and copper wire was connected to the anode. Once the AC applied, the light illumed as shown in Figure 5b. With finger curving and the strain of hydrogel increasing up to 50%, negligible changes in the light brightness could be observed during finger movement (**Video 2**). This artificial ligament is able to continuously transmit steady AC electronic signal without degradation of continuous finger movements, and such signal could be used to monitor the ligament condition regardless of mechanical deformations. The white dash line indicates the position of hydrogel wire which have been inserted inside the robotic finger.

A robotic system was built (**Figure S18**) to further demonstrate the robotic artificial nerve applications. This hydrogel and the pressure sensor were integrated and a LED were used as the indicator. The system was supplied with DC; if no pressure is applied to the pressure sensor, no current could be measured. Once pressed the pressure sensor, a sharp and large current was detected at the beginning and then decreased soon to a certain value (Figure 5c). Once the strain of the hydrogel increased to 100%, the current responses show a similar trend to that of 0% strain, while obvious decreases in both the peak and steady-state of currents could be observed, which is consistent with the discussion in Figure 3a.

As shown in Figure 5d, when no pressure is loaded on the pressure sensor, the whole system is open circuited. Therefore, the LED on the robot finger turns off (Figure 5d (ii)). Once the pressure sensor is touched with a human finger, which applies a certain level of pressure. The resistance of the sensor and the current through the artificial nerve are obviously reduced to

trigger the LED (Figure 5d (iii)). This system can generate different touching signals with different finger position (different hydrogel strain).

3. Conclusion

In conclusion, we have fabricated a novel natural rubber-like ionic conductive hydrogel by infiltrating HPC fibers embedded PVA hydrogel with NaCl solution. This hydrogel is biocompatible, stretchable (fully recover under 100% strain), and combines tunable mechanical strength (from 0.6 to 4 MPa tensile strength), good elasticity (from 15 to 900 kPa), large strain (up to 975%), and high ionically conductivity (up to 3.4 S m^{-1} at f = 1 MHz). HPC fibers play a critical role in increasing Na^+ and Cl^- ions concentration and provide large space for ionic migration. To the best of our knowledge, the balanced mechanical strength, elongation, and elasticity of stretchable hydrogel with high conductivity are important for artificial tissue usage, but hard to be achieved at the same time. The ionic conductive hydrogel wire is successfully fabricated and embedded in 3D printed robotic hand to demonstrate as an artificial nerve, which enables passing stable AC and tunable DC electrical signals as well as full recovery under robotic finger movement. Our design is versatile and adaptable to a variety of hydrogels and ionic liquids/solutions for soft and stretchable conductive gels.

4. Experimental Section

Fabrication of HPC/PVA ionic conductive conductor: Polyvinyl alcohol (PVA, Mw ~61,000, Sigma-Aldrich), Hydroxypropyl cellulose (HPC, Mw ~100,000, 99% purification, Sigma-Aldrich), dimethyl sulfoxide (DMSO, analysis purification, Sigma-Aldrich), sodium chloride (NaCl, 99%, Sigma-Aldrich) and Deionized water (18.2 MΩ). All chemicals were without further purification.

Firstly, 0.9 mL of DMSO was added into 3 mL of deionized water, followed by 0.1 g HPC and the mixture was stirred for 10 minutes. Next, the mixture was heated up to 70 °C using a water bath for further stirring until all HPC was fully dissolved. Then 0.64 g PVA was added

afterward, and the mixture was heated up again to 90 °C until all PVA powders were dissolved, and then continue heating and stirring for 3 hours. Then the HPC/PVA solution was poured into a mold to cool down to room temperature for 12 hours. At the same time, the cooling prcocess will eliminate the visible gas bubbles in solution due to stirring (**Figure S19**). Then the HPC/PVA solution was frozen in fridge at -20 °C. It was taken out of the fridge after 12 hours of freezing and thawed for 3 hours. After 3 freeze-thaw cycles, a solid HPC/PVA hydrogel was obtained. By varying the ratio of PVA weight percentage, three kinds of hydrogels HPC/PVA_x were produced (x refers to the weight ratio: 4, 8 and 16). Then HPC/PVA_x hydrogel was soaked in NaCl solution (concentration from 1 to 5M) for 12 hours (ions exchanging reached equilibrium after soaking 12 hours, Table S1) to generate HPC/PVA_x ionic conductive hydrogel. **Figure S20** shows the whole process to generate the PVA based ionic conductive hydrogel.

Fabrication of pressure sensor: The pressure sensors were reported in our previous work.[30] Microstructured AgNWs/PDMS films were prepared by depositing an aqueous solution of AgNWs (Blue Nano) on silicon masters and allowing this to dry in air, and then casting a mixture of PDMS elastomer and crosslinker in 10:1 (w/w) ratio (Sylgard 184, Dow Corning) through spin-coating (1000 rpm). The elastomer mixture was degassed in a vacuum and cured at 90 °C for 1 h, then the films were sectioned by a scalpel and peeled off from the silicon master. The microstructured AgNWs/PDMS film is then placed face-to-face with an interdigital gold electrode to form a resistive pressure sensor.

Mechanical properties characterization: The hydrogels were prepared in a rectangular shape (3.2 mm x 2.2 mm x 25 mm) for tensile testing. All measurements were taken with MTS C43 machine. A fixed rate of extension (2 mm min^{-1}) was applied to all tensile testing. The nominal stress (σ) was calculated by dividing the applied force (F) by the cross-section area, and the nominal tensile strain (ε) was obtained by dividing stretched length (Δl) by the original length (l_0). The elastic module was obtained from the stress-strain curve and the toughness was the total area under the stress-strain curve. The elastic modulus was calculated from the slope over

0 ~ 100% of strain ratio of the stress-strain curve. The toughness was calculated from the area of stress-strain curves. For recovery experiment, we prepared five groups of hydrogel samples were 10 s, 30 s, 60 s, and 300 s, respectively. These samples were firstly extended to 300% strains and then placed for a different time for recovery. For loading-unloading tests, the dissipated energy was calculated by **Equation 1**:

$$U_i = \int_{loading} \sigma d\varepsilon - \int_{unloading} \sigma d\varepsilon \quad (1)$$

Where σ and ε are tensile stress and strain during the cycles.

Electrical characterizations: The AC signals were generated by function/arbitrary waveform generator (Agilent 33220A) and were measured by an oscilloscope (Tektronix DPO5054B). The electrical measurements for control of robotic hands were characterized by Keithley 4200 semiconductor characterization system.

Optical characterization: JSM-5310 and FESEM-6340F were used to capture the scanning electron microscope (SEM) and energy-dispersive X-ray spectroscopy (EDX) images of the sample. Before the experiment, samples were freeze-dried using liquid nitrogen (N_2) before drying in a chamber for 72 hours. After that, the freeze-dried powder was examined using SEM. The Fourier transform infrared spectroscopy (FTIR) data was collected by FTIR Perkin Elmer Spectrophotometer (Spectrum 400 FT-IR). The height distributions of HPC/PVA hydrogel were obtained by Zeiss Smartproof 5 optical surface profiler. All the microscope images were obtained through the Olympus BX51 microscope.

Supporting Information

Supporting Information is available from the Wiley Online Library or from the author.

Acknowledgements

Yang Zhou, and Changjin Wan contributed equally to this work. This research is supported by grants from the National Research Foundation, Prime Minister's Office, Singapore under its Campus of Research Excellence and Technological Enterprise (CREATE) programme,

Ministry of Education (MOE) Tier one, RG124/16 and RG200/17. The characterization of SEM and XRD were performed at the Facility for Analysis Characterization Testing & Simulation (FACTS) in Nanyang Technological University, Singapore.

Received: ((will be filled in by the editorial staff))
Revised: ((will be filled in by the editorial staff))
Published online: ((will be filled in by the editorial staff))

References

[1] a) C. Keplinger, J.-Y. Sun, C. C. Foo, P. Rothemund, G. M. Whitesides, Z. Suo, Science 2013, 341, 984; b) M. L. Hammock, A. Chortos, B. C. K. Tee, J. B. H. Tok, Z. Bao, Adv. Mater. 2013, 25, 5997; c) M. Ramuz, B. C. K. Tee, J. B. H. Tok, Z. Bao, Adv. Mater. 2012, 24, 3223; d) D. Qi, Z. Liu, Y. Liu, Y. Jiang, W. R. Leow, M. Pal, S. Pan, H. Yang, Y. Wang, X. Zhang, J. Yu, B. Li, Z. Yu, W. Wang, X. Chen, Adv. Mater. 2017, 29, 1702800; e) G. Chen, N. Matsuhisa, Z. Liu, D. Qi, P. Cai, Y. Jiang, C. Wan, Y. Cui, W. R. Leow, Z. Liu, S. Gong, K.-Q. Zhang, Y. Cheng, X. Chen, Adv. Mater. 2018, 30, 1800129.
[2] a) D.-H. Kim, N. Lu, R. Ma, Y.-S. Kim, R.-H. Kim, S. Wang, J. Wu, S. M. Won, H. Tao, A. Islam, K. J. Yu, T.-i. Kim, R. Chowdhury, M. Ying, L. Xu, M. Li, H.-J. Chung, H. Keum, M. McCormick, P. Liu, Y.-W. Zhang, F. G. Omenetto, Y. Huang, T. Coleman, J. A. Rogers, Science 2011, 333, 838; b) T. Sekitani, T. Someya, in *Stretchable Electronics*, Wiley-VCH Verlag GmbH & Co. KGaA, 2012, 271.
[3] a) R. Pelrine, R. Kornbluh, Q. Pei, J. Joseph, Science 2000, 287, 836; b) S. J. Benight, C. Wang, J. B. H. Tok, Z. Bao, Prog. Polym. Sci. 2013, 38, 1961.
[4] a) B. Hu, C. Owh, P. L. Chee, W. R. Leow, X. Liu, Y.-L. Wu, P. Guo, X. J. Loh, X. Chen, Chem. Soc. Rev. 2018; b) C. Li, M. J. Rowland, Y. Shao, T. Cao, C. Chen, H. Jia, X. Zhou, Z. Yang, O. A. Scherman, D. Liu, Adv. Mater. 2015, 27, 3298; c) A. V. Salvekar, W. M. Huang, R. Xiao, Y. S. Wong, S. S. Venkatraman, K. H. Tay, Z. X. Shen, Acc. Chem. Res. 2017, 50, 141; d) M. D. Konieczynska, M. W. Grinstaff, Acc. Chem. Res. 2017, 50, 151; e) F. Zhang, L. Xiong, Y. Ai, Z. Liang, Q. Liang, Adv. Sci. 2018, 5, 1800450.
[5] a) C. Y. Tay, Y.-L. Wu, P. Cai, N. S. Tan, S. S. Venkatraman, X. Chen, L. P. Tan, NPG Asia Mater. 2015, 7, e199; b) I. Irwansyah, Y.-Q. Li, W. Shi, D. Qi, W. R. Leow, M. B. Y. Tang, S. Li, X. Chen, Adv. Mater. 2015, 27, 648; c) Y. Hu, W. Guo, J. S. Kahn, M. A. Aleman-Garcia, I. Willner, Angew. Chem., Int. Ed. 2016, 55, 4210.
[6] B. Jeong, Y. H. Bae, D. S. Lee, S. W. Kim, Nature 1997, 388, 860.
[7] a) Y. Ke, C. Zhou, Y. Zhou, S. Wang, S. H. Chan, Y. Long, Adv. Funct. Mater. 2018, 28, 1800113; b) Y. Zhou, M. Layani, S. Wang, P. Hu, Y. Ke, S. Magdassi, Y. Long, Adv. Funct. Mater. 2018, 28, 1705365.
[8] R. Langer, D. A. Tirrell, Nature 2004, 428, 487.
[9] A. T. Neffe, B. F. Pierce, G. Tronci, N. Ma, E. Pittermann, T. Gebauer, O. Frank, M. Schossig, X. Xu, B. M. Willie, M. Forner, A. Ellinghaus, J. Lienau, G. N. Duda, A. Lendlein, Adv. Mater. 2015, 27, 1738.
[10] P. Calvert, Adv. Mater. 2009, 21, 743.
[11] a) P. Thoniyot, M. J. Tan, A. A. Karim, D. J. Young, X. J. Loh, Adv. Sci. 2015, 2, 1400010; b) K. Haraguchi, T. Takehisa, Adv. Mater. 2002, 14, 1120.

[12] a) J. P. Gong, Y. Katsuyama, T. Kurokawa, Y. Osada, Adv. Mater. 2003, 15, 1155; b) A. Nakayama, A. Kakugo, J. P. Gong, Y. Osada, M. Takai, T. Erata, S. Kawano, Adv. Funct. Mater. 2004, 14, 1124.
[13] a) J.-Y. Sun, X. Zhao, W. R. K. Illeperuma, O. Chaudhuri, K. H. Oh, D. J. Mooney, J. J. Vlassak, Z. Suo, Nature 2012, 489, 133; b) X. P. Morelle, W. R. Illeperuma, K. Tian, R. Bai, Z. Suo, J. J. Vlassak, Adv. Mater., 1801541; c) C. H. Yang, B. Chen, J. Zhou, Y. M. Chen, Z. Suo, Adv. Mater. 2016, 28, 4480; d) M. Wehner, R. L. Truby, D. J. Fitzgerald, B. Mosadegh, G. M. Whitesides, J. A. Lewis, R. J. Wood, Nature 2016, 536, 451.
[14] a) M. J. d. Silva, A. O. Sanches, L. F. Malmonge, J. A. Malmonge, Mater. Res. 2014, 17, 59; b) J. R. May, C. Gentilini, D. E. Clarke, Y. I. Odarchenko, D. V. Anokhin, D. A. Ivanov, K. Feldman, P. Smith, M. M. Stevens, RSC Adv. 2014, 4, 2096; c) V. R. Feig, H. Tran, M. Lee, Z. Bao, Nat. Commun. 2018, 9, 2740.
[15] B. Depalle, Z. Qin, S. J. Shefelbine, M. J. Buehler, J. Mech. Behav. Biomed. Mater. 2015, 52, 1.
[16] W.-K. Shin, J. Cho, A. G. Kannan, Y.-S. Lee, D.-W. Kim, Sci. Rep. 2016, 6, 26332.
[17] a) S. Yao, Y. Zhu, Adv. Mater. 2015, 27, 1480; b) J. Wang, C. Yan, G. Cai, M. Cui, A. Lee-Sie Eh, P. See Lee, Adv. Mater. 2016, 28, 4490; c) T. Sekitani, T. Someya, Adv. Mater. 2010, 22, 2228; d) Y. Cao, T. G. Morrissey, E. Acome, S. I. Allec, B. M. Wong, C. Keplinger, C. Wang, Adv. Mater. 2017, 29, 1605099; e) S. Z. Bisri, S. Shimizu, M. Nakano, Y. Iwasa, Adv. Mater. 2017, 29, 1607054.
[18] J. Odent, T. J. Wallin, W. Pan, K. Kruemplestaedter, R. F. Shepherd, E. P. Giannelis, Adv. Funct. Mater. 2017, 27, 1701807.
[19] J. P. Gong, Y. Katsuyama, T. Kurokawa, Y. Osada, Adv. Mater. 2003, 15, 1155.
[20] a) C. Marin, E. Fernández, Front. Neuroeng. 2010, 3, 8; b) E. Castagnola, A. Ansaldo, E. Maggiolini, T. Ius, M. Skrap, D. Ricci, L. Fadiga, Front. Neuroeng. 2014, 7.
[21] T. Ito, Y. Yeo, C. B. Highley, E. Bellas, C. A. Benitez, D. S. Kohane, Biomaterials 2007, 28, 975.
[22] C. Wu, N. Yosef, T. Thalhamer, C. Zhu, S. Xiao, Y. Kishi, A. Regev, V. K. Kuchroo, Nature 2013, 496, 513.
[23] W. E. Hennink, C. F. van Nostrum, Adv. Drug Delivery Rev. 2002, 54, 13.
[24] K. Missoum, J. Bras, M. N. Belgacem, Biomacromolecules 2012, 13, 4118.
[25] S. Komiya, E. Otsuka, Y. Hirashima, A. Suzuki, Prog. Nat. Sci.: Mater. Int. 2011, 21, 375.
[26] Z. Zhao, H. Chen, H. Zhang, L. Ma, Z. Wang, Biosens. Bioelectron. 2017, 91, 306.
[27] A. van Boxtel, Psychophysiology 2001, 38, 22.
[28] a) Y. Ding, J. Zhang, L. Chang, X. Zhang, H. Liu, L. Jiang, Adv. Mater. 2017, 29, 1704253; b) Y. Gu, S. Zhang, L. Martinetti, K. H. Lee, L. D. McIntosh, C. D. Frisbie, T. P. Lodge, J. Am. Chem. Soc. 2013, 135, 9652; c) S. Liu, O. Oderinde, I. Hussain, F. Yao, G. Fu, Polymer 2018, 144, 111; d) D. Kim, J. Park, J. H. Kim, Y.-C. Kang, H. S. Kim, Thin Solid Films 2018, 646, 92.
[29] a) T. Li, S. Xiang, P. Ma, H. Bai, W. Dong, M. Chen, J. Polym. Sci., Part B: Polym. Phys. 2015, 53, 1020; b) J. Yang, C. R. Han, J. F. Duan, M. G. Ma, X. M. Zhang, F. Xu, R.-C. Sun, Cellulose 2013, 20, 227; c) K. Shi, Z. Liu, Y.-Y. Wei, W. Wang, X.-J. Ju, R. Xie, L.-Y. Chu, ACS Appl. Mater. Interfaces 2015, 7, 27289; d) Y. Sun, S. Liu, G. Du, G. Gao, J. Fu, Chem. Commun. 2015, 51, 8512; e) S. Sornkamnerd, M. K. Okajima, T. Kaneko, ACS Omega 2017, 2, 5304; f) G.-l. Du, Y. Cong, L. Chen, J. Chen, J. Fu, Chin. J. Polym. Sci. 2017, 35, 1286; g) M. Sabzi, N. Samadi, F. Abbasi, G. R. Mahdavinia, M. Babaahmadi, Mater. Sci. Eng., Proc. Conf. 2017, 74, 374; h) Y. Liu, M. Zhu, X. Liu, W. Zhang, B. Sun, Y. Chen, H.-J. P. Adler, Polymer 2006, 47, 1.
[30] B. Zhu, H. Wang, Y. Liu, D. Qi, Z. Liu, H. Wang, J. Yu, M. Sherburne, Z. Wang, X. Chen, Adv. Mater. 2016, 28, 1559.

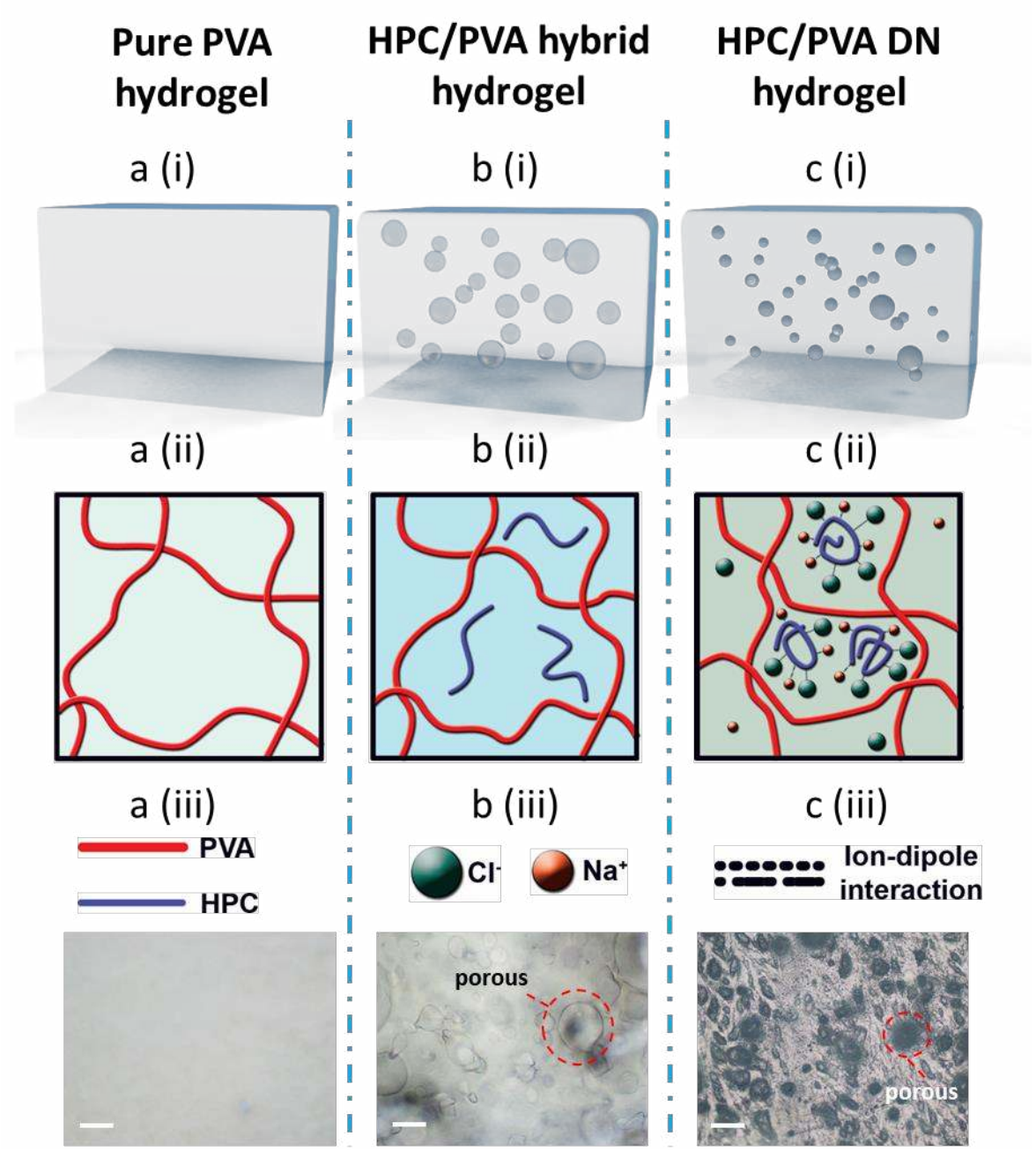

Figure 1. (i) Schematic design, (ii) microstructure and (iii) microscope image, respectively, of a) pure PVA (16 wt%) hydrogel, where pure PVA hydrogel has uniform structure; b HPC/PVA (2.5/16 wt%) hybrid hydrogel, where HPC fibers dispersed inside of PVA hydrogel matrix, and water porous generated around HPC fibers inside of PVA hydrogel matrix; c) HPC/PVA (2.5/16 wt%) ionic conductive hydrogel (soaked in 5M NaCl solution), whereas Na^+ and Cl^- ions were attracted by HPC fibers through ion-dipole interaction, and porous in HPC/PVA ionic conductive hydrogel were kept. The scale bar of microscope-images is 100 μm.

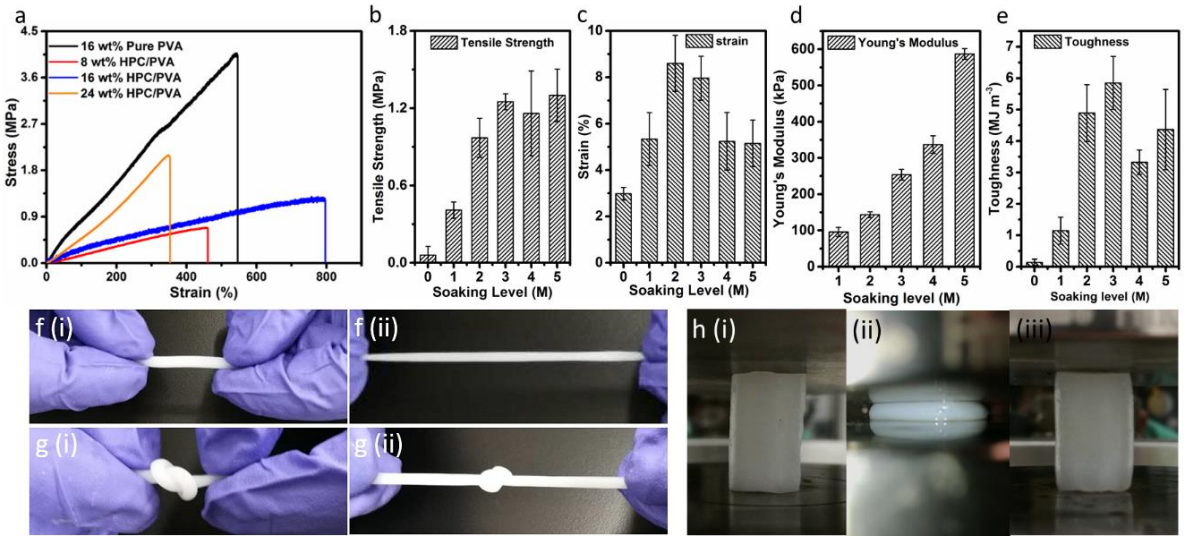

Figure 2. a) Tensile curves of HPC/PVA hydrogel with different PVA wt% and pure PVA hydrogel as reference at 3M soaking level b) tensile strength, c) strain, d) Young's modulus and e) toughness of HPC/$PVA_{16\%}$ ionic conductive hydrogel with different ionic concentration from 1 to 5M, f) stretching, g) knotting and h) compression of HPC/$PVA_{16\%}$ ionic conductive hydrogel.

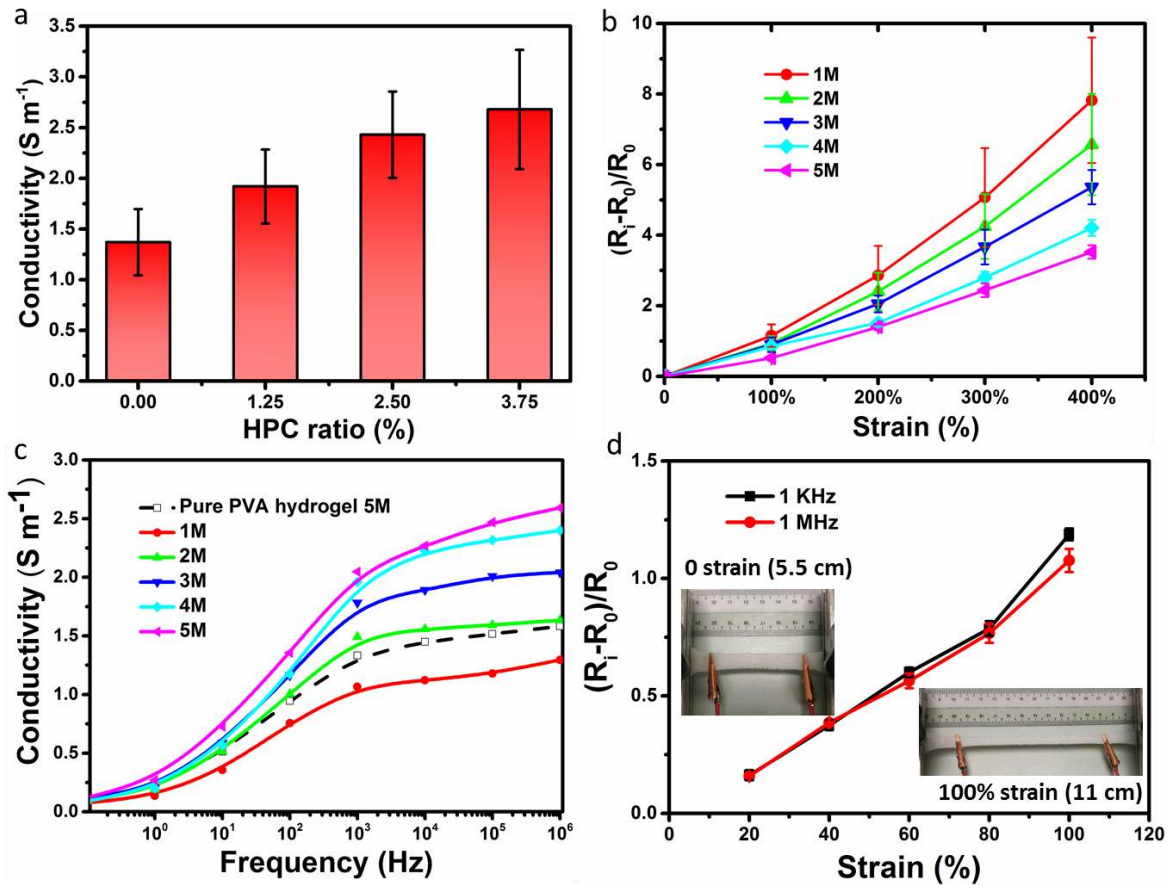

Figure 3. a) Ionic conductivity of HPC/PVA ionic conductive hydrogel increases with increasing HPC ratio, b) Gauge factor of HPC/PVA ionic conductive hydrogel increases with increasing of strain from 0 to 400% or decreasing of soaking level form 5M to 1M, c) ionic conductivity HPC/PVA ionic conductive hydrogel increases

with both AC frequency soaking level increasing, c) relative change in hydrogel resistance of AC, the insert photos are HPC/PVA ionic conductive hydrogel at 0 and 100% strain.

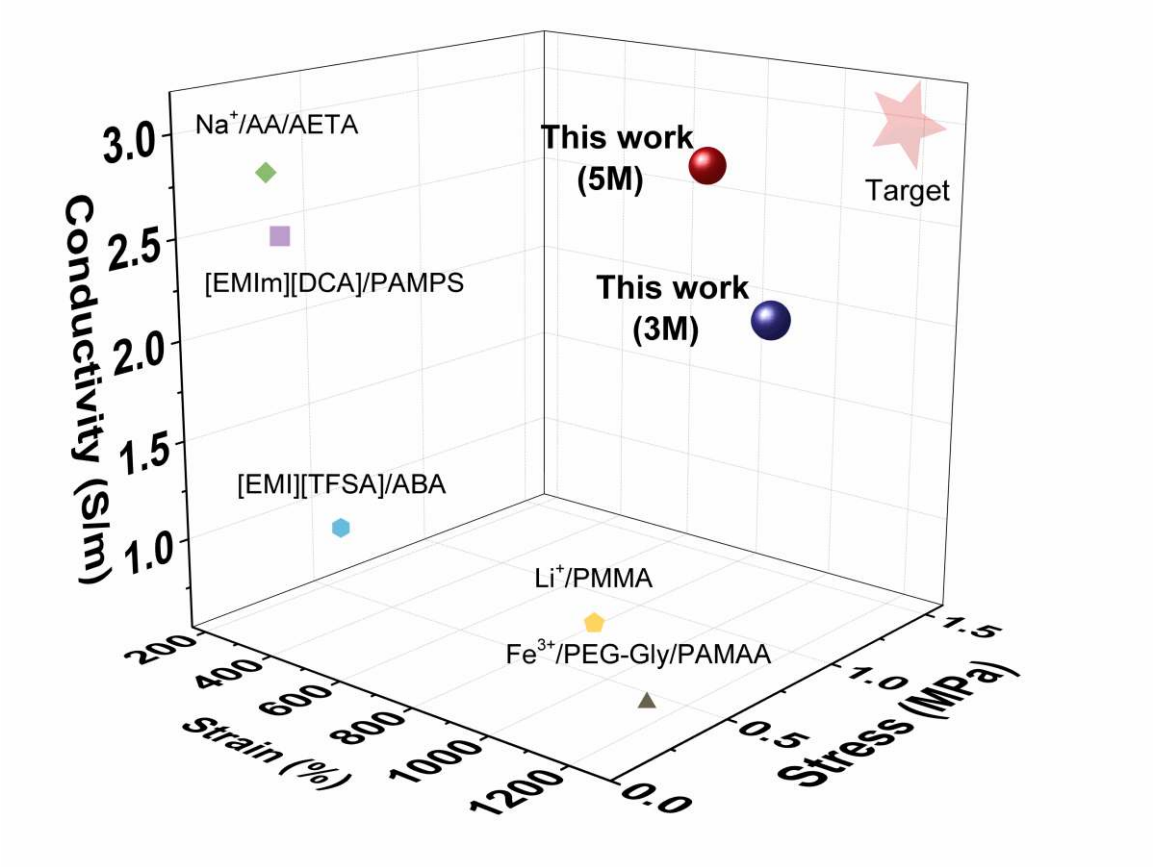

Figure 4. Comparison of strain, stress and conductivity of reported ionic conductive gels including: [EMIm][DCA]/PAMPS,[28a] Na^+/AA/AETA,[18] Fe^{3+}/PEG-Gly/PAMAl[28c], [EMI][TFSA]/ABA,[28b] and Li^+/PMMA based gel,[28d] and HPC/PVA ionic conductive hydrogel (3M, 5M).

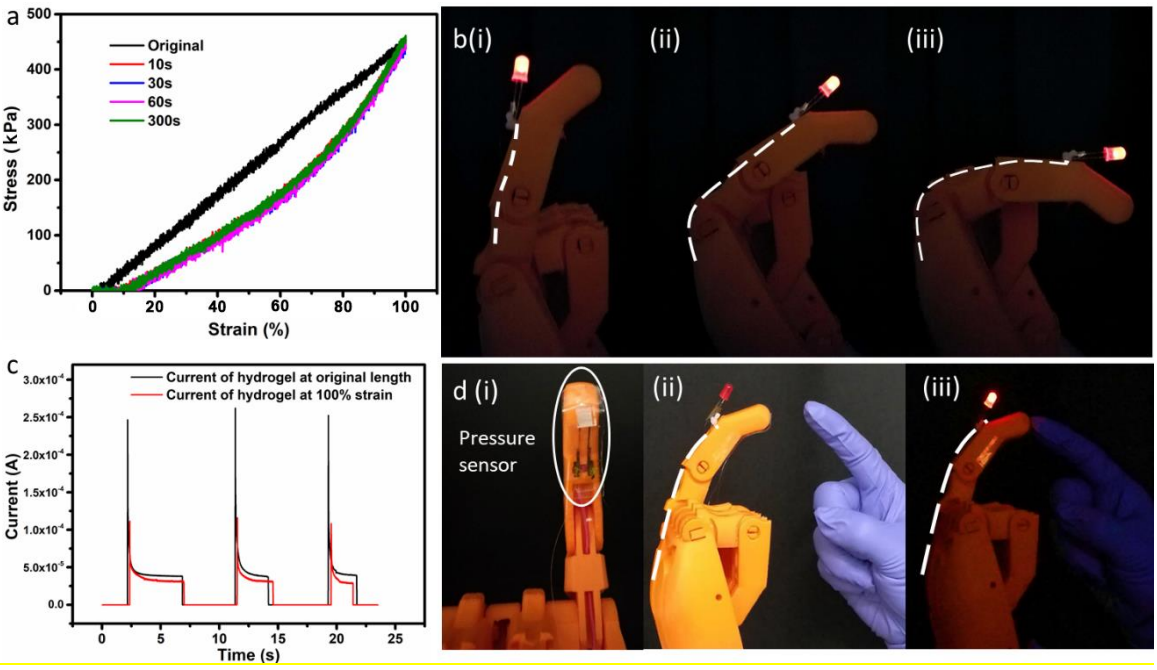

Figure 5. a) Self-recovery of HPC/PVA ionic conductive hydrogel, b) demonstration of hydrogel system on robotic hand with AC applied to transfer steady AC signal, c), response of hydrogel and pressure sensor integrated

system when loading a 2 kPa pressure collected at different strain 0% and 50%, d) demonstration of hydrogel/sensor system on robotic hand with DC applied.

The table of contents

A simple method was developed to introduce ions rich pores into strong hydrogel matrix and fabricate a novel ionic conductive hydrogel with a high level performance of both electronic and mechanical properties, which have great potential for stretchable electronics and artificial tissue applications

Keyword: Tough hydrogel, ionic conductive hydrogel, soft electronics, bioelectronics, tissue engineering

Y. Zhou, C. Wan, Y. S. Yang, H. Yang, S. Wang, Z. Dai, K. Ji, H. Jiang, X. Chen*, and Y. Long*

Highly Stretchable, Elastic, and Ionic Conductive Hydrogel for Artificial Soft Electronics

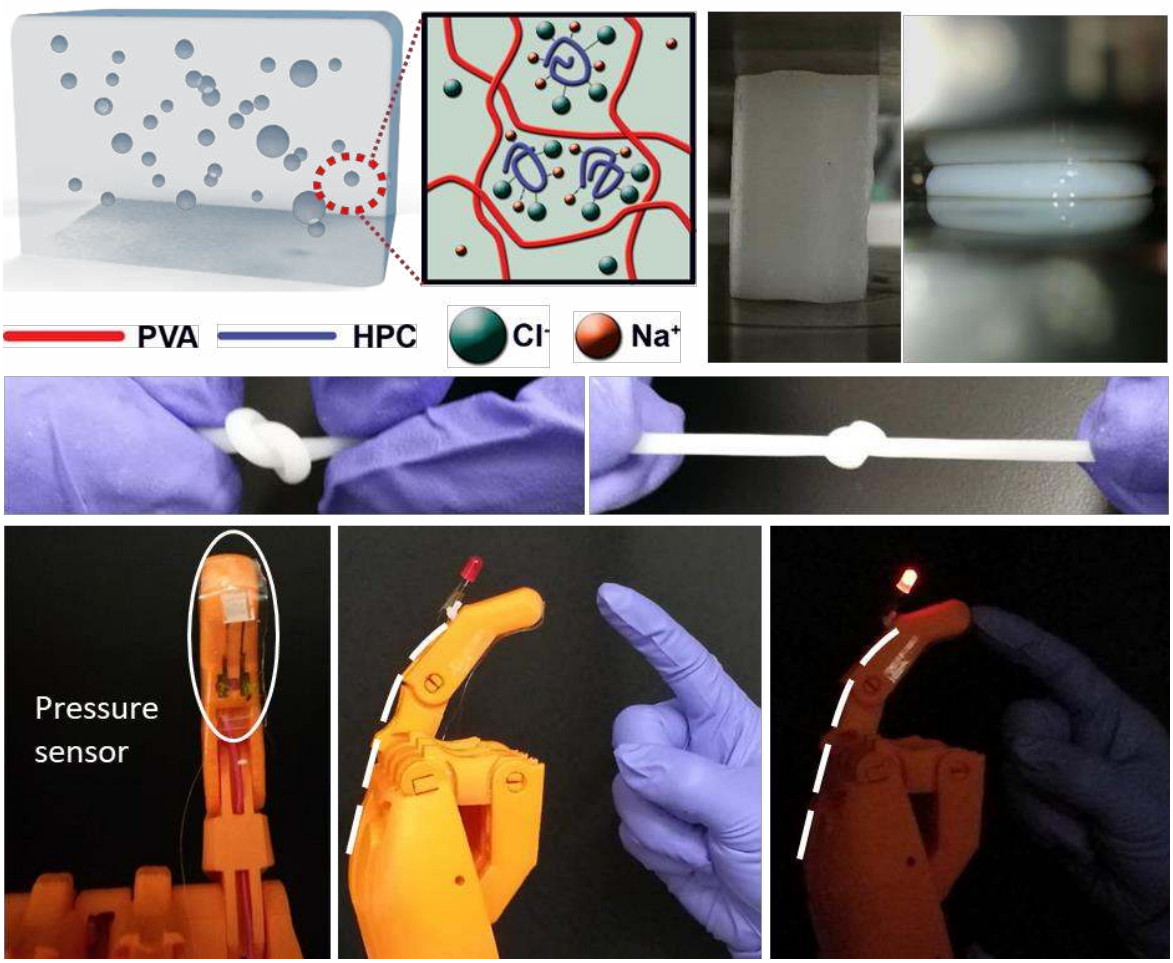

Supporting Information

Highly Stretchable, Elastic, and Ionic Conductive Hydrogel for Artificial Soft Electronics

Yang Zhou, Changjin Wan, Yongsheng Yang, Hui Yang, Shancheng Wang, Zhendong Dai, Keju Ji, Hui Jiang, Xiaodong Chen, and Yi Long**

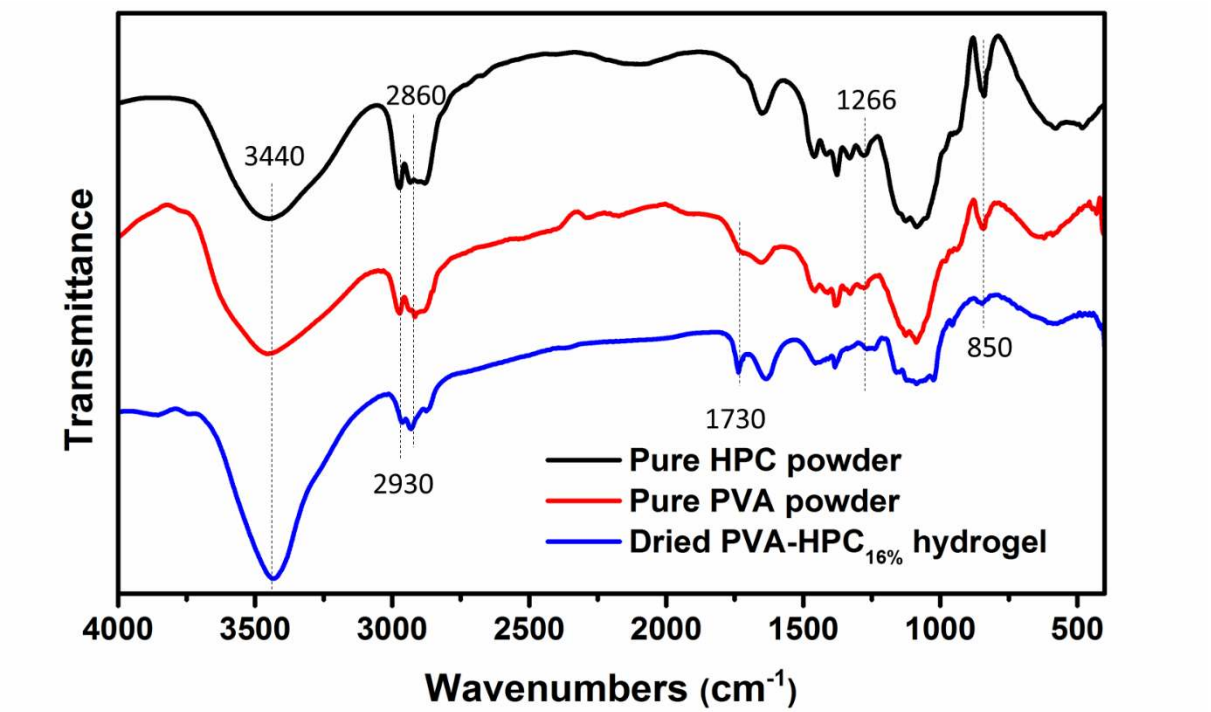

Figure S1. FTIR spectrums commercial HPC fibers (black), PVA powders (red), and dried HPC/PVA hydrogel sample (blue). As shown in the spectra of all the three samples, the following significant peaks can be observed in all the three samples. The broad peak at 3440 cm^{-1} assigned to the O-H stretching vibration. The absorption band at 2930 cm^{-1} and a shoulder at 2860 cm^{-1} correspond to the stretching of -CH_2- and -CH-, respectively. The band at 1450 cm^{-1} is attributed to -CH_2- bending. Moreover, the bands shown 1266 cm^{-1} is due to -CO- stretching. The band at 850 cm^{-1} is attributable to rocking vibration of the methylene groups. Furthermore, the band at 1730 cm^{-1} just can be observed in PVA powder and HPC/PVA hydrogel correspond to the unhydrolyzed acetate groups. All of the significant peaks of dried HPC/PVA hydrogel can be observed in commercial PVA and HPC powders' FTIR spectra, which indicated that HPC didn't interact with PVA, and no chemical reaction happened during the gelation process[1, 2].

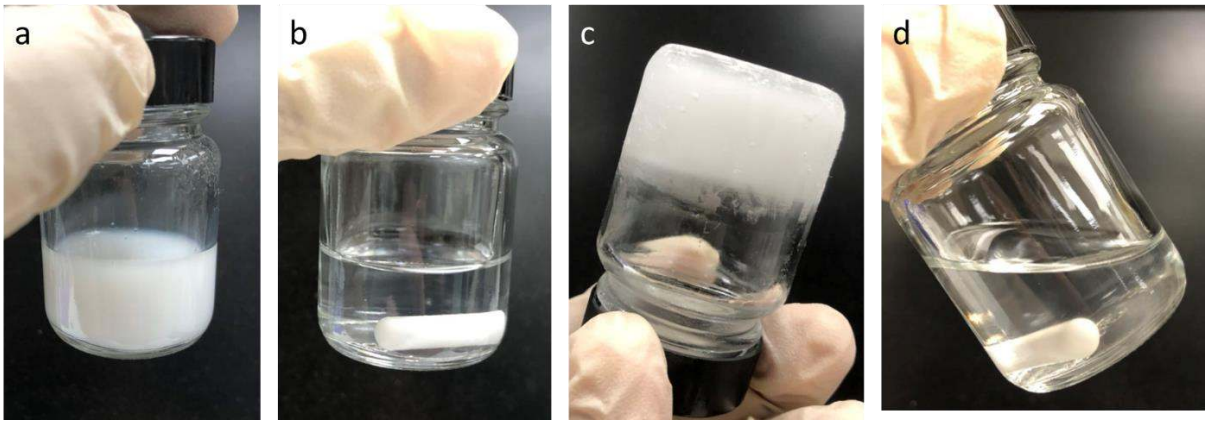

Figure S2 Pure HPC solution a) after stirring and heating process, b) after cooling down in room temperature for 12 hours, c) after freezing in fridge at -20 °C for 12 hour, d) after 3 freeze-thaw cycles at room temperature.

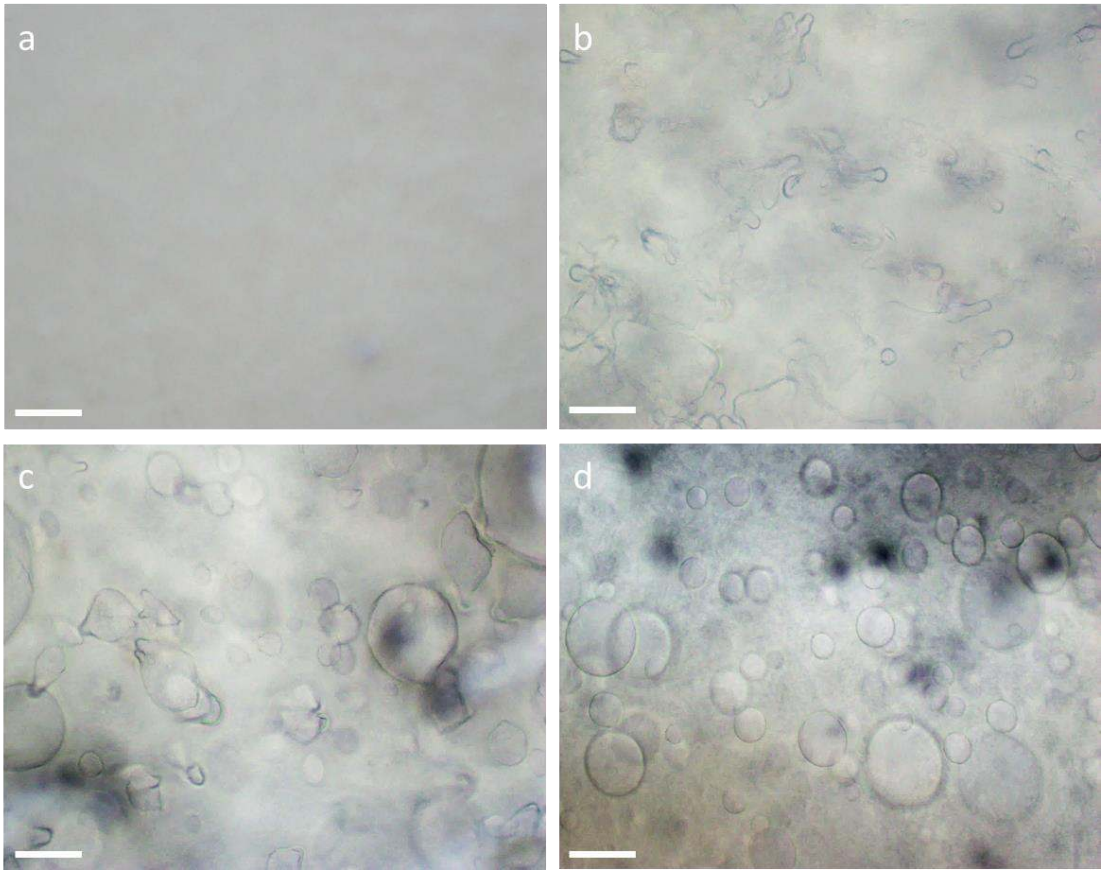

Figure S3. Microscope images of HPC/PVA hydrogel with different HPC ratio: a) 0 wt%, b) 1.25 wt%, c) 2.50 wt% and d) 3.75 wt% .

Figure S4. a) PVA-HPC$_{16\%}$ hydrogel, b) PVA-HPC ionic conductive hydrogel (soaked in 5M NaCl solution). After soaking in saturated NaCl solution for 24 hours, volume of PVA-HPC$_{16\%}$ hydrogel decreased from 364 mm^3 to 214 mm^3. PVA-HPC$_{16\%}$ hydrogel is totally transparent, while PVA-HPC ionic conductive hydrogel is translucent.

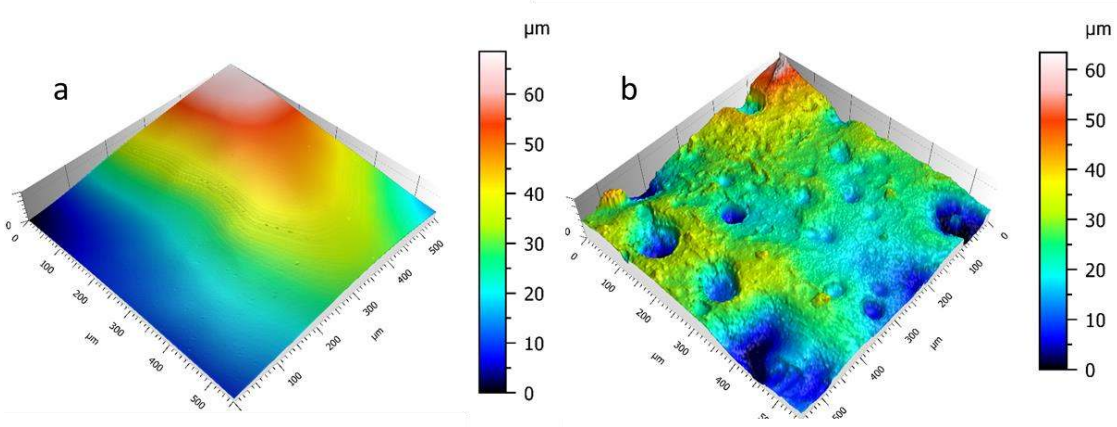

Figure S5. Height distribution images by optical surface profiler of HPC/PVA hydrogel before (a) and after (b) soaking in NaCl solution (5M).

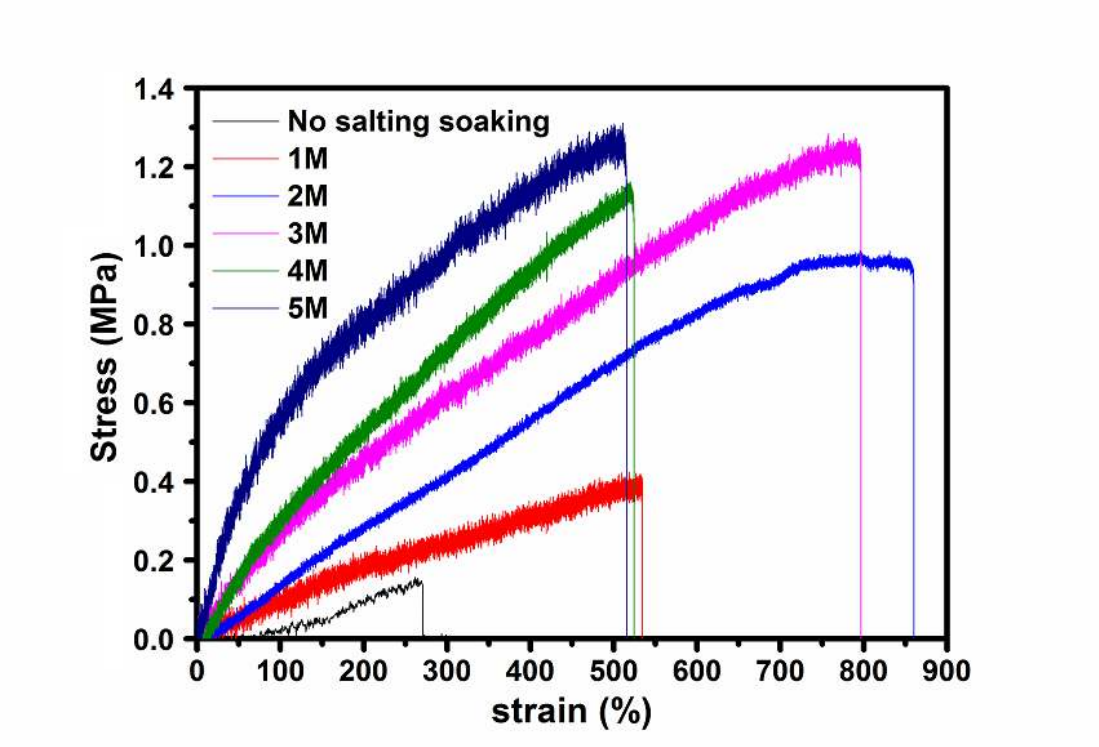

Figure S6. Tensile strength curve of PVA-$HPC_{16\%}$ ionic conductive hydrogel in soaking NaCl solutions with different concentration from 1 to 5M.

Figure S7. Load-bearing capacity of HPC/PVA ionic conductive hydrogel (3M) (2 mm thickness, 5 mm width).

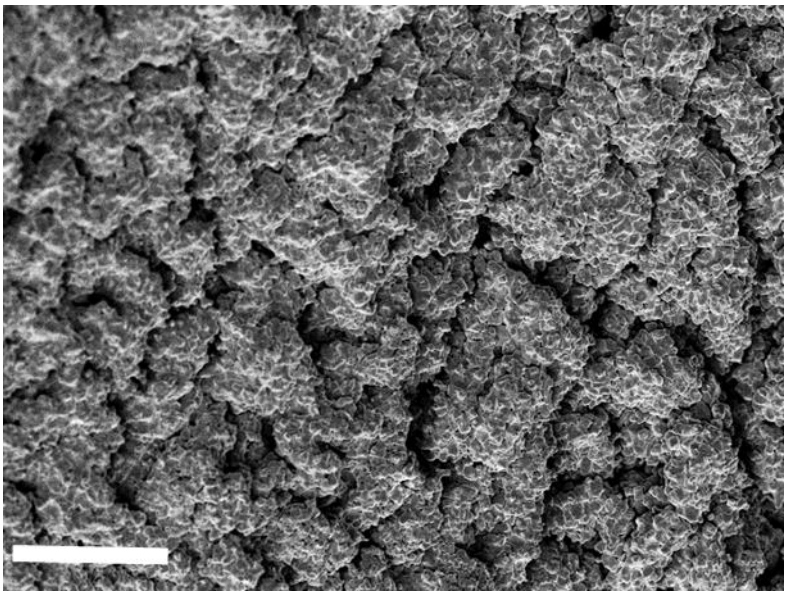

Figure S8. SEM-image of Freeze-dried HPC/PVA ionic conductive hydrogel (scale bar is 10 μm).

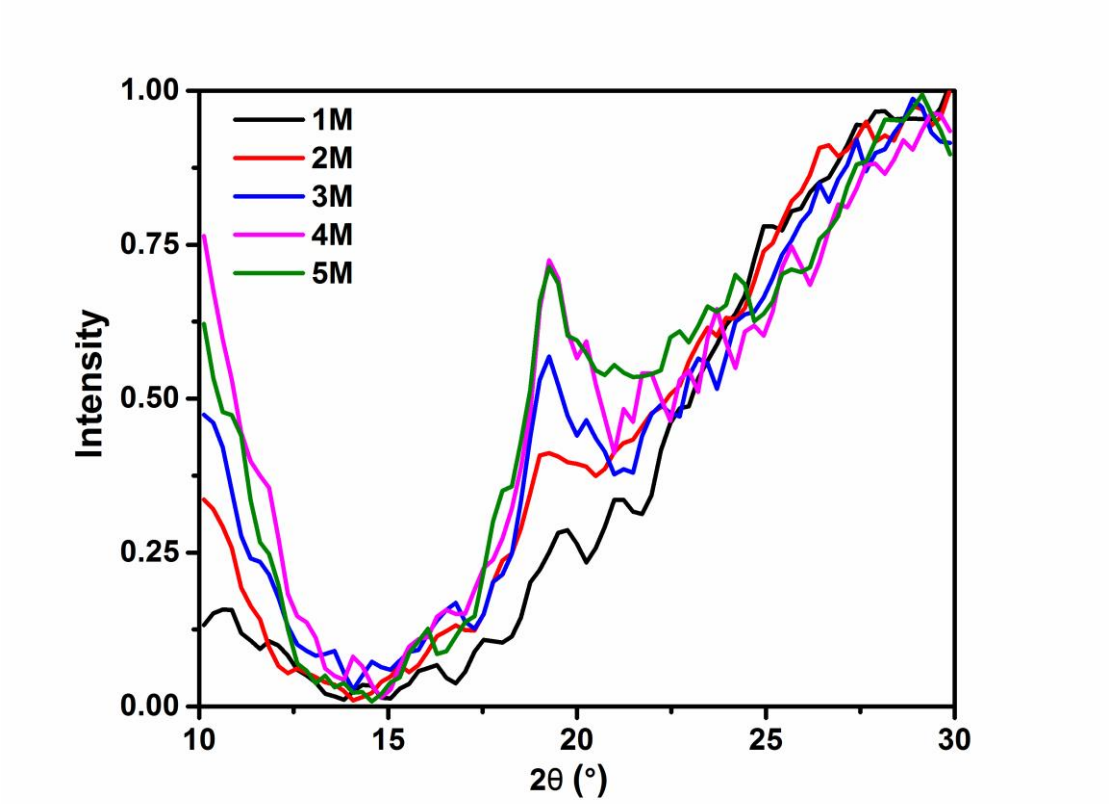

Figure S9. XRD spectra of PVA-HPC ionic conductive hydrogels after soaking in NaCl solution with different concentration from 1 to 5M.

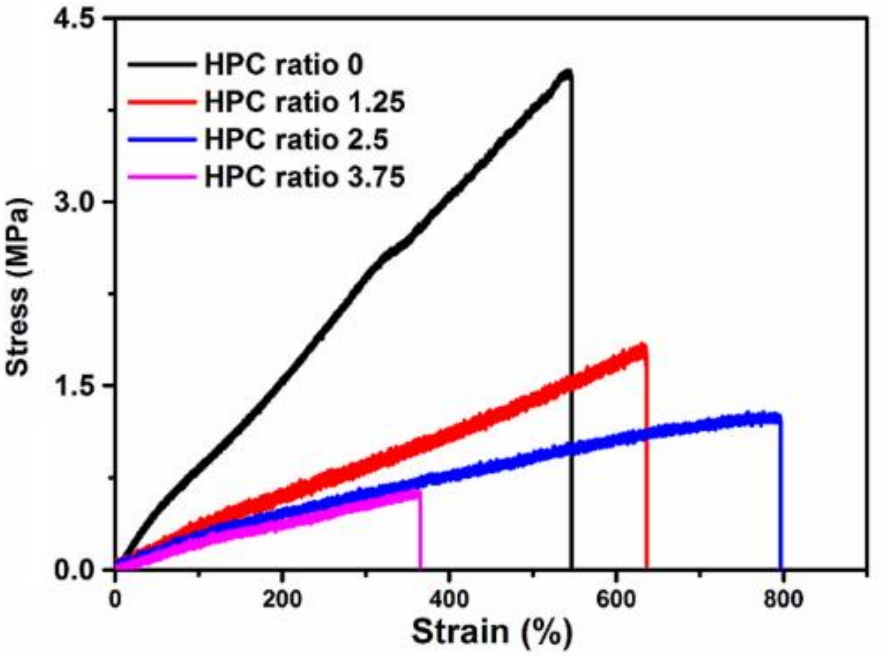

Figure S10. Tensile strength curve of HPC/PVA ionic conductive hydrogel after soaking in NaCl solutions (3M) with increasing HPC ratio from 0 to 3.75 wt%.

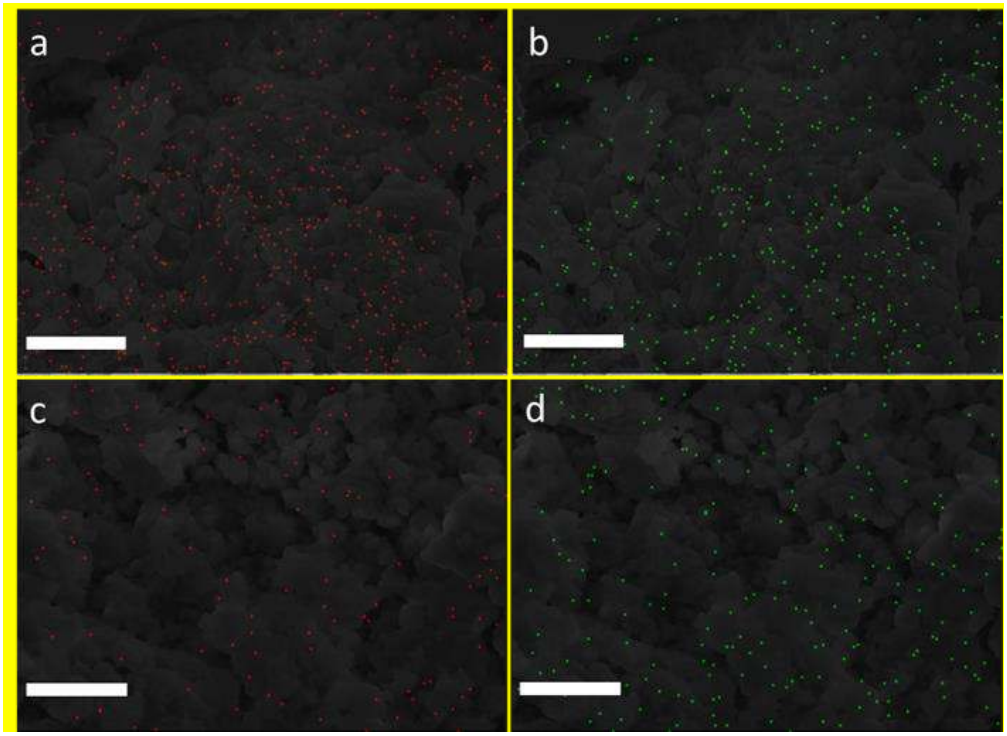

Figure S11. a) Na^+ and b) Cl^- on the cut surface of freeze-dried HPC/PVA ionic conductive hydrogel; c) Na^+ and d) Cl^- on the cut surface of freeze-dried pure PVA ionic conductive hydrogel (scale bar is 10 μm).

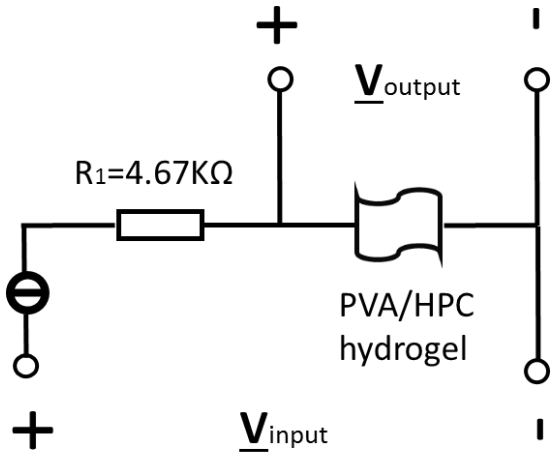

Figure S12. Circuit for resistance characteristic under strain.

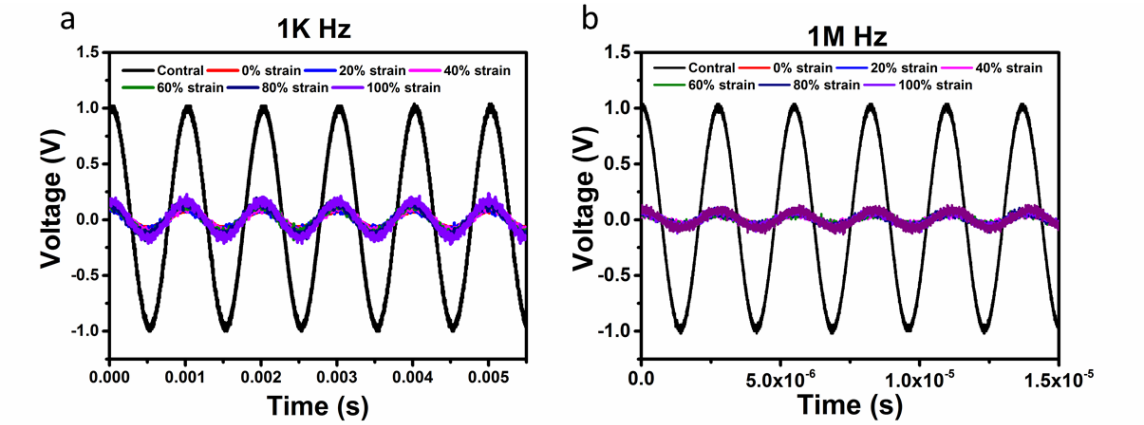

Figure S13. Circuit for resistance characteristic under strain, AC signal of hydrogel a) 1 kHz and b) 1 MHz, respectively.

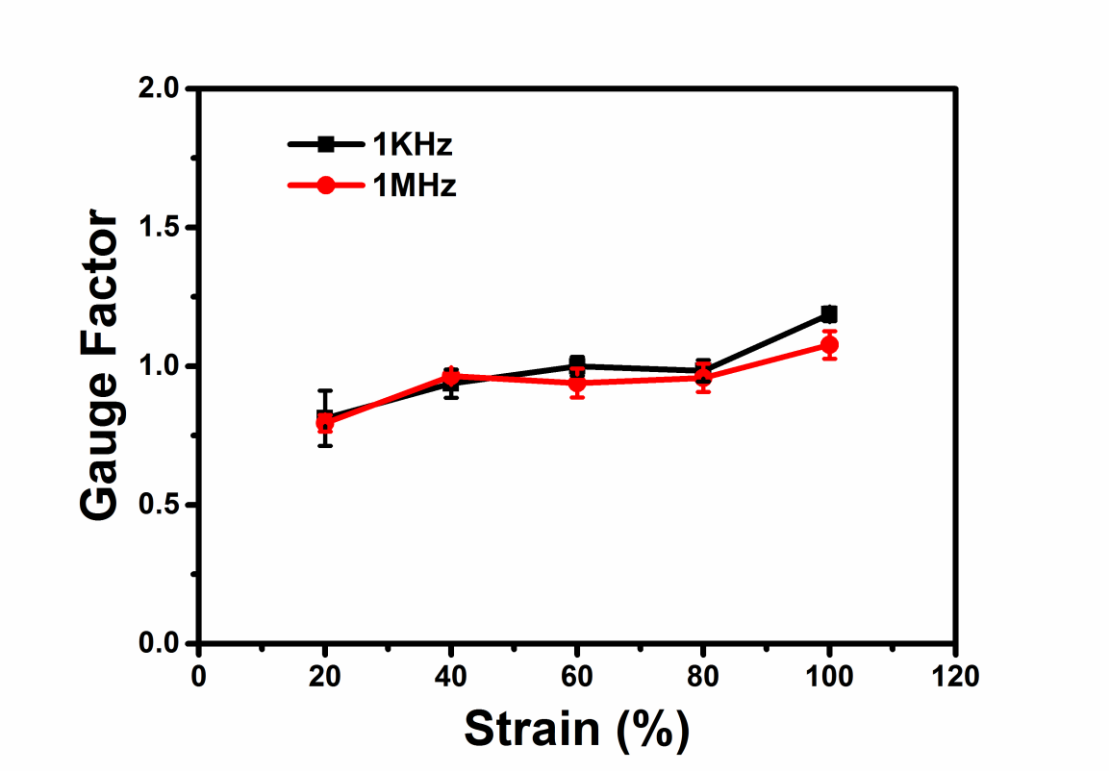

Figure S14. Relative change in hydrogel gauge factor of AC at both 1 kHz and 1 MHz.

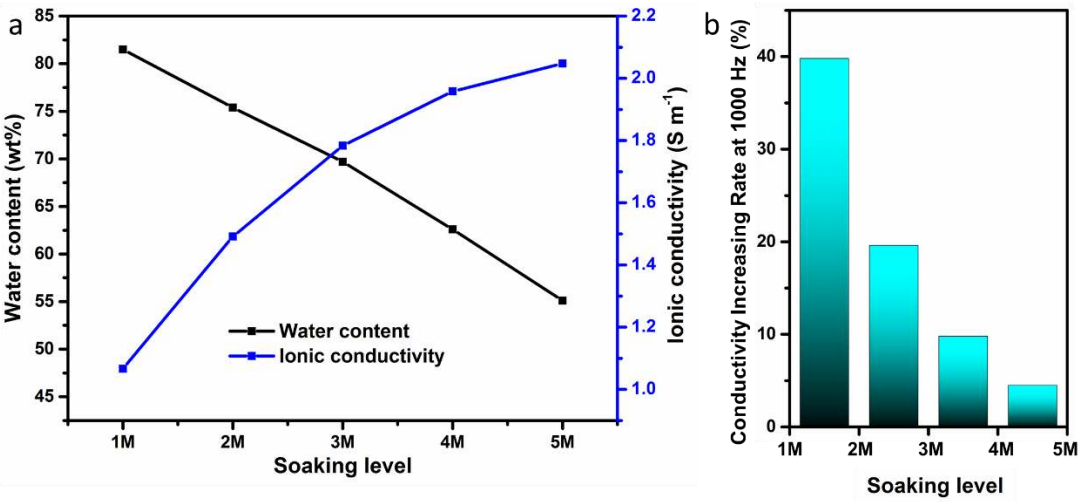

Figure S15 a) Trend of Water content (black) and ionic conductivity (blue) with soaking level increasing from 1~5M, b) Conductivity increasing rate trend. The conductivity increasing rate (I) was calculated as: $I_i^{i+1} = (C_{i+1}-C_i)/C_i \times 100\%$, where C_i represent the conductivity of HPC/PVA ionic conductive hydrogel at iM soaking level; I_i^{i+1} represent the conductivity increasing rate between iM and i+1M soaking level.

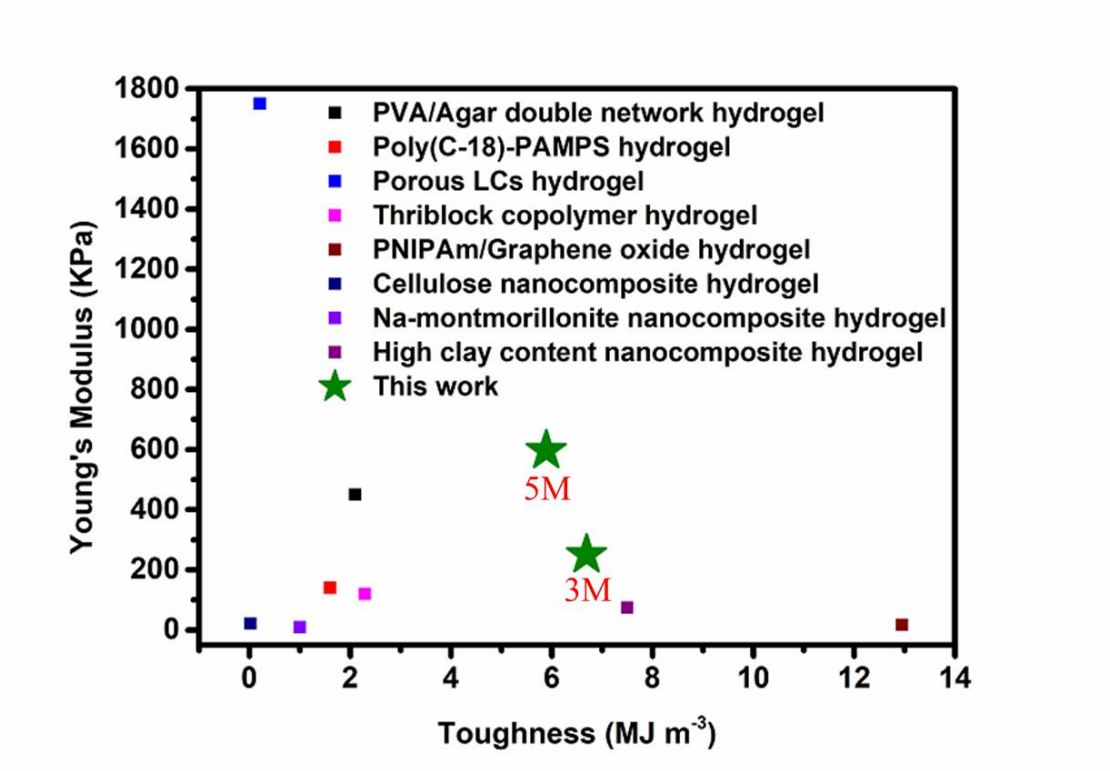

Figure S16. Comparison of toughness and young's modulus of hydrogels have potential to be used in artificial tissue applications and HPC/PVA ionic conductive hydrogel.

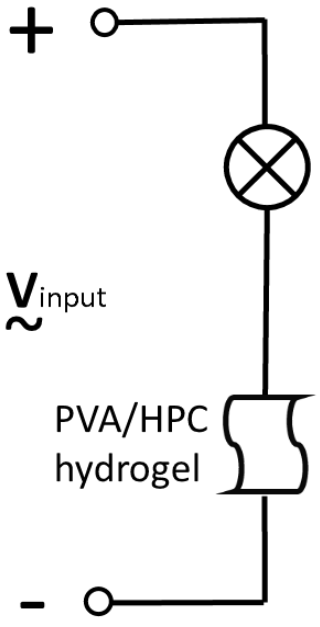

Figure S17. Circuitry design of steady AC demonstration.

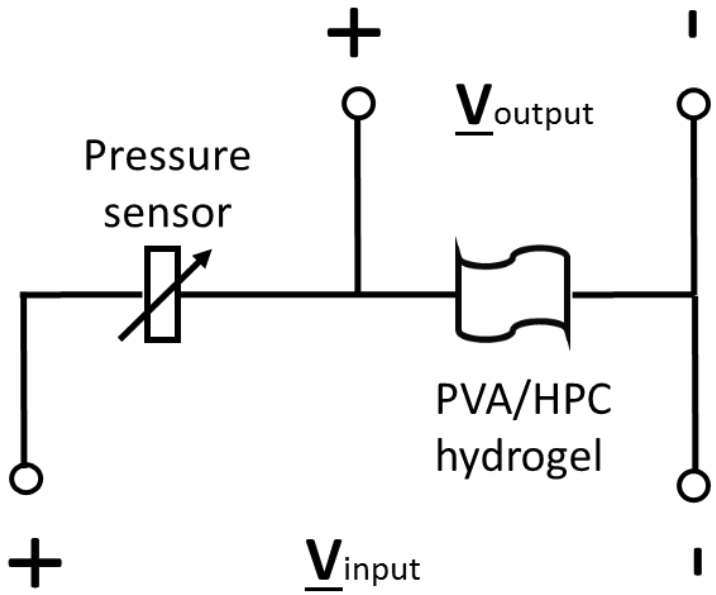

Figure S18. Circuitry design of hydrogel and pressure sensor system for DC-compression demonstration.

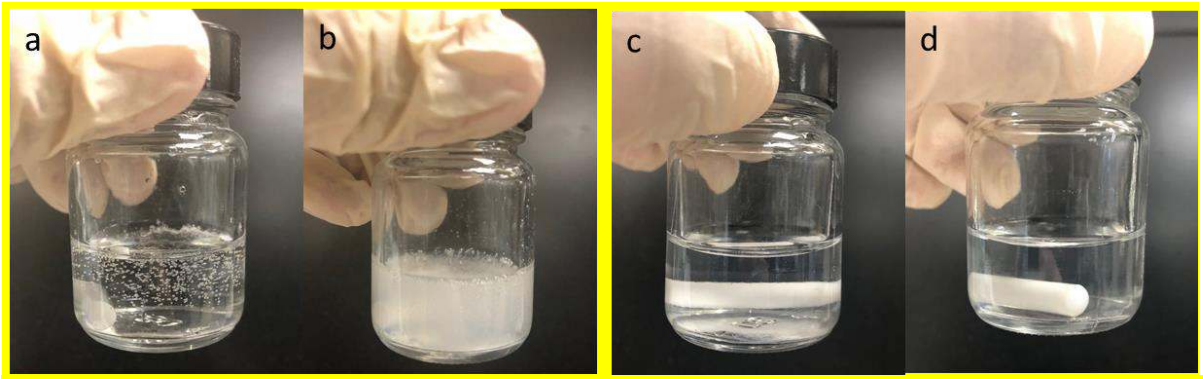

Figure S19. a) Pure PVA solution and b) HPC/PVA solution after heating and stirring immediately; c) Pure PVA solution and b) HPC/PVA solution after degassing for 12 hours at room temperature, no visible bubbles can be observed in both solutions.

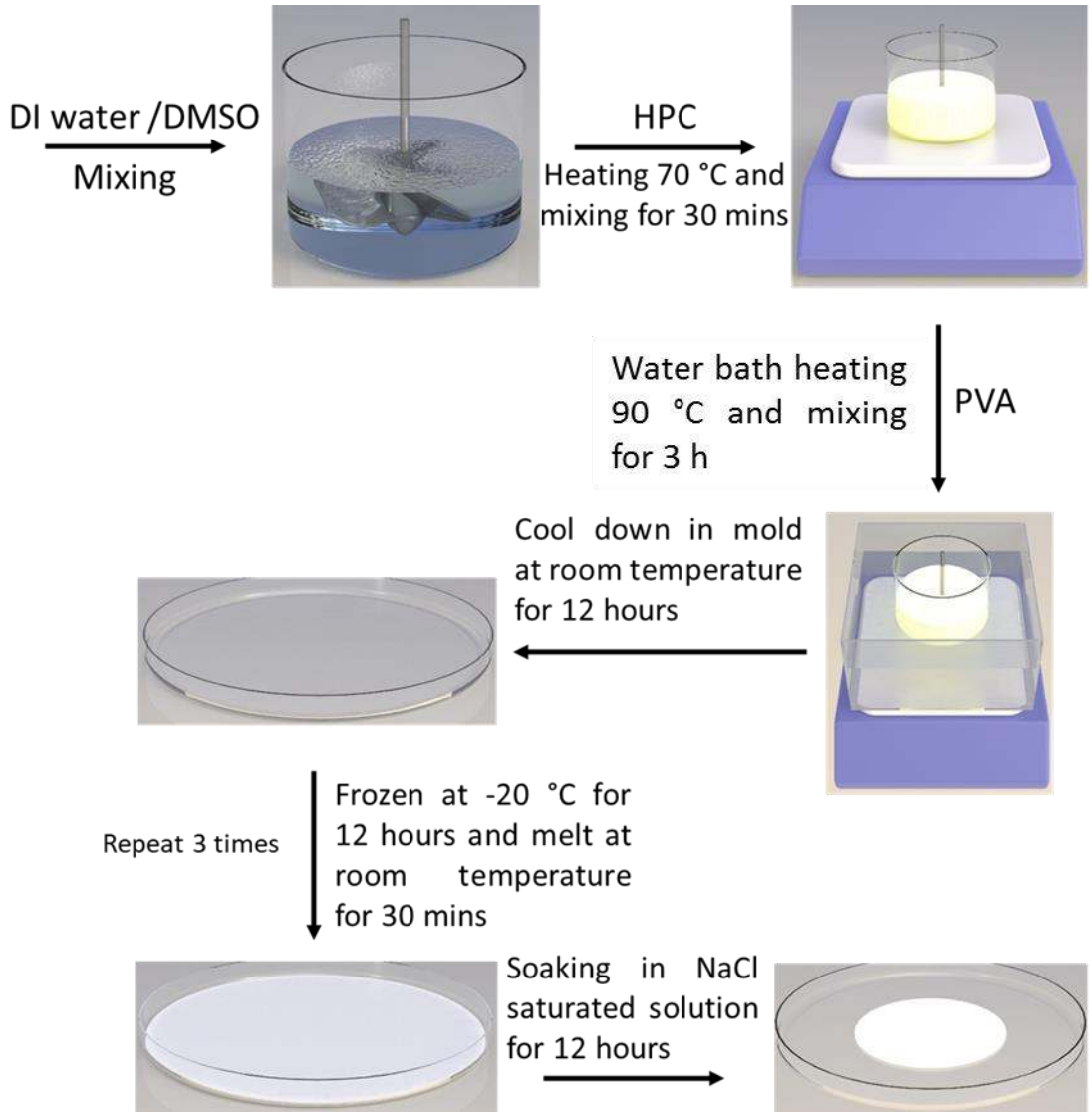

Figure S20. Gelation process of converting HPC/PVA composite hydrogel to ionic conductive hydrogel.

Table S1 Weight change (%) of HPC/PVA hydrogel soaking in 1~5M solution after 12, 24 and 36 hours. (All the samples weight normalized as 100% by the weight of the sample soaked after 12 hours)

	12 h	24 h	36 h
1M	100%	99.96%	99.68%
2M	100%	99.60%	98.99%
3M	100%	100.3%	99.42%
4M	100%	100.3%	99.8%
5M	100%	99.34%	99.25%

References

[1] C. A. Finch, *Polyvinyl Alcohol--Developments*, 2nd Edition ed.; Willey and Sons, **1992.**

[2] D. An, D. Zhao, X. Li, X. Lu, G. Qiu, K. J. Shea, *Carbohydr. Polym.* **2015,** *134*, 385.